INTER-AMERICAN TROPICAL TUNA COMMISSION

SCIENTIFIC ADVISORY COMMITTEE

13TH MEETING

(by videoconference)
16-20 May 2022

DOCUMENT SAC-13 INF-M

COMPARISON OF INDICES OF ABUNDANCE FOR THE SOUTH EPO SWORDFISH STOCK IN THE EQUATORIAL AREA

Carolina Minte-Vera, Haikun Xu, Sung-Il Lee, Hirotaka Ijima, Cleridy Lennert-Cody, Mark N. Maunder

ABSTRACT

Due to its wide temporal and spatial distribution, the catch and effort data from the Japanese fleet has been used in past assessments to derive indices of abundance for the south EPO swordfish stock. The Japanese index computed for the 2011 assessment has shown an increase, which has continued into the 2022 index (SAC-13-INF-N). There is anecdotical information that the fleet may have incorporated the use of light-sticks, and changed its secondary target to swordfish, which may have changed the catchability, but no related data are available. In this document we construct indices of abundance using spatiotemporal models for swordfish based on the Korean and the Japanese longline data, in the equatorial area, where the fleets' operations overlap the most in the EPO, between 10°N and 15°S, 110°W and 150°W, with the goal of better understanding why the Japanese index has increased in recent years and what factors may be affecting the estimates of swordfish density. The indices derived from the two fleets showed striking similarities until 2010 not only between them but also with an index derived from the New Zealand fleet. After 2010, the Japanese index increases even further, especially in the fourth quarter of every year, while the Korean index stays stable. The differences are discussed based on three hypotheses: changes in availability, biased imputation due to preferential sampling, change in catchability. Further work should extend this analysis into the WCPO.

INTRODUCTION

Indices of abundance should be the most important information used to fit integrated stock assessment models, after catches (Francis 2011). Well-constructed indices provide information on trends in abundance, and in combination with catches, may provide information on absolute abundance. Ideally, indices should be derived from well-designed fishery-independent surveys and should be an accurate representation of the population. For swordfish stocks, like for tunas and other wide-range tuna-like species, there are no fishery-independent surveys. Indices of abundance are obtained from longline catch and effort data, which are standardized statistically by fitting models that include covariates that represent factors that affect catchability (*e.g.,* gear configuration, vessel identification, environmental factors, season, and location of operation).

For swordfish in the Pacific Ocean, the first challenge in obtaining an index of abundance is the uncertainty in the stock structure, which results in overlapping stock boundaries for the different assessments. The IATTC 2011 assessment assumed the stock to be distributed south of 5°S and east of 150°W. The 2021 WCPFC assessment considered the southwestern Pacific Ocean stock to be distributed south of the equator in the western and central Pacific Ocean and to extend to the EPO, south of 4°S between 150°W and 130°W, and. The new south EPO assessment is expected to consider catches taken south of 10°N and east of 150°W (SWO-01). This new assumption for assessment boundaries allows for the comparison of indices from the Korean and Japanese data in the equatorial area, where the operation of the two longline fleets overlap. The equatorial area is also a location of interest where the swordfish catches have increased considerably in the last 10 years (SAC-13-09).

Although it is unknown to what extent the operation of each fleet overlaps with the spatial distribution of the south EPO stock because of the uncertainty in the stock structure, the Japanese data has been used to derive indices of abundance for the S EPO stock because it has a widespread area of operation and a long time of operation in the region. The Japanese index computed for the 2011 assessment has shown an increase (SAC-02-09), which has continued into the 2022 index (SAC-13-INF-N). There is anecdotical information that the fleet may have incorporated the use of light-sticks, and changed its secondary target to swordfish, which may have changed the catchability, but no related data are available. To explore the hypothesis that the increase in the Japanese index maybe due to change in catchability due to potential changes in fishing strategy by the Japanese fleet, indices obtained from the Japanese and the Korean fleets were compared. We constructed indices for the equatorial area, where the fleets' operations overlap the most in the EPO, between 10°N and 15°S, 110°W and 150°W. In the 1960's, its area of operation extended from the IATTC management boundary at 150°W all the way east to the coast of the Americas, but over time, the fleet has increasingly operated only in the western region of the EPO. The Korean fleet has a more constrained area of operation than the Japanese fleet and in recent years has tended to operate in the equatorial areas in the vicinity of the Antigua Convention boundary at 150°W.

DATA

The available catch and effort data are the operational-level data for the Korean longline fleet operating in the Pacific Ocean for 1974 to 2018 (obtained through a Memorandum of Understanding with the National Institute of Fisheries Science, NIFS), and the 1° latitude by 1° longitude by month and category of hooks-between-float (HBF) data for the Japanese fleet for 1994 to 2020 (obtained from the annual submission of the CPCs in compliance with the IATTC resolution C-03-05 on the provision of data, catch and effort level 2 data). Length-frequency data are available for both the Korean and the Japanese fleet, but the coverage of those data in space and time is sparse. Only data from 1994 to 2018 were included in both models due to the temporal availability of data for both fleets. The operational level data for Korea were aggregated into a 1° by 1° area by quarter by HBF resolution. The Japanese data were aggregated by quarter. The area of operation of both fleets has contracted over time, but with different patterns (Figure 1). In the EPO, the Japanese fleet contracted its operation mainly to the equatorial area and to the southeast of the EPO, off Chile (south of 20°S and east of 100°W). The Korean area of operation contracted towards the vicinity of the central Pacific Ocean. No data west of 150°W were available for Japan.

Only one gear configuration covariate was included in the models: hooks between floats (HBF). For use in the models, the HBF variable was treated as a categorical variable into three levels: (11-14], (14,17], (18,20]. There were not enough sets with HBF values outside of this range to be included in the analysis (Figure 2).

The area chosen for this study is from 10°N to 15°S and 150°W to 110°W, where the operations of the two fleets overlap the most in the EPO. Within this study area, only 1° areas ("cells") that had more than 3 "observations" (combinations of HBF category and month) for both Korean and Japan were included in the model for each fleet (Figure 3).

The available length-frequency data are coarse and sparse in space and time for both fleets (see Figure 9 top panel), and are not split by HBF category. Preliminary spatiotemporal models including these data did not converged due likely to the coarse spatial and temporal resolution of the data. Therefore, simple averages of the length-frequencies by year and quarter were used to represent the standardized CPUE.

The indices were compared to the nominal CPUE (sum of catches over sum of effort) and to the index obtained for the New Zealand fleet for the SW Pacific Ocean (Finucci et al, 2021). The index for New Zealand comes from the standardization of the operational-level longline data from the New Zealand fleet, which operates north of 45°N and south of 30°S between 180° and 170°E (=190°W). The standardization model included several operational variables such as night fraction (fraction of the set soak time during the hours of darkness), and number of light sticks, which were important predictors of the CPUE. The series "All Vessels Long Index" (in Table 3.2 of Finucci et al. 2021) was use for the comparisons.

METHODS

We modelled the catch and effort of each fleet using a vector-autoregressive spatiotemporal model implemented in the VAST R library (Thorson and Barnett, 2017). The use of spatial-temporal models, to deal with changes in the spatial distribution of the fishery and the stock, has been considered one of the best ways to standardize catch and effort data to produce indices of abundance and to standardize age/size composition data to produce composition associated with those indices (Xu et al 2019, Maunder et al 2020). The VAST model allows for the estimation of spatial and spatio-temporal correlations that with some assumptions, can be used to predict density for unfished areas, and implements an area-weighted estimate of density as the way of computing the abundance index.

A delta-lognormal generalized linear mixed model was fit to each data set, with a binomial function assumed for the presence-absence and a lognormal function assumed for the positive CPUE values. The correlation structure for the encounter probability and for the positive catch rate had two components: a time-invariant spatial one and a time-varying spatiotemporal one. The fixed effects are the independent temporal effects (year.quarter) and the independent effect of the catchability covariate, HBF. The model was fit using the R VAST library version v13_0_0 (Thorson and Barnett, 2017)

The encounter probability (p) for observation i is modeled using a using a logit-linked linear predictor:

$$\text{logit}(p_i) = \beta_1(t_i) + \lambda_1 + L_{\omega 1}\omega_1(s_i) + L_{\varepsilon 1}\varepsilon_1(s_i, t_i) \qquad \text{(Equation 1)}$$

and the positive catch rate (λ) for observation i is modeled using a log-linked linear predictor:

$$\log(\lambda_i) = \beta_2(t_i) + \lambda_2 + L_{\omega 2}\omega_2(s_i) + L_{\varepsilon 2}\varepsilon_2(s_i, t_i) \qquad \text{(Equation 2)}$$

In the above equations, $\beta_x(t_i)$ is the intercept for in year t_i, and λ_x is the effect of the covariate HPB on catchability, $\omega_x(s_i)$ is time-invariant spatial variations at location s_i, $\varepsilon_x(s_i,t_i)$ is the time-varying spatiotemporal variations at location s_i in year t_i, $L_{\omega x}$ and $L_{\varepsilon x}$, are the scaling coefficients of the random effect distributions, for each linear predictor $x=1$ encounter probability and $x=2$ positive catch rate. Vessel effects were not included because the information was only available for the Korean fleet.

Both the spatial and spatiotemporal random effects are assumed to be positively correlated in space; that is, the closer the locations, the higher their similarities in density and encounter probability. The random effects are assumed to have a multivariate normal distribution with mean vector equal zero and variance-covariance matrix R_x, thus for spatial random effects:

$$\omega_1(s_i) \sim MVN(0, R_1) \quad \text{(Equation 3a)}$$

$$\omega_2(s_i) \sim \text{MVN}(0, R_2) \quad \text{(Equation 3b)}$$

and for spatiotemporal random effect:

$$\varepsilon_1(s_i, t_i) \sim MVN(0, R_1) \quad \text{(Equation 4a)}$$

$$\varepsilon_2(s_i, t_i) \sim MVN(0, R_2) \quad \text{(Equation 4b)}$$

where R_1 and R_2 are variance-covariance matrices parametrized using the Matérn correlation function that predicts a smooth decrease in correlation between values of separate locations according to distance. In this application anisotropy was assumed: decline in correlation depends also on the direction of the distance (Thorson et al., 2015, Thorson 2020).

The spatial locations are also named "knots". For each observation, all spatial variables have their values equal to the value at the location of the nearest knot. The number of knots, which was chosen to be 100 for this application, implicitly defined the spatial resolution at which the estimated of spatial variation in the population are done. The position of the knots is defined by VAST using a K-means algorithm to minimize the distance between samples and knots. In this application, the information was aggregated at a 1° by 1° by quarter resolution. The spatial domain was on the order of 40° in the longitude axis x 25° in the latitude axis, equal to one thousand 1° by 1° cells per quarter, thus about 10 cell per knot.

To assess the performance of the final model, visual inspection of the quantile residuals was done (Dunn and Smyth, 1996; Hartig, 2020).

The final indices of abundance are estimated by summing the product of knot-specific density and the area of the knot and correcting for biases (Thorson and Kristensen, 2016).

RESULTS AND DISCUSSION

The nominal CPUE increases over time for both the Korean and the Japanese fleet in each of the HBF categories and subareas (Figure 4). Both models show a strong correlation of density in the east-west direction (Figure 5), which corresponds to the direction of the dominant currents operating in the area (Kessler, 2006). The quantile residuals showed uniform distribution over the catchability covariate (Figure 6 top) and that strong spatial pattern in the quantile residuals is not apparent (Figure 6 bottom and Appendix 1), as would be expected if the data were adequately modelled (Hartig, 2020). The difference between the nominal and standardized indices are greatest for quarter 4 after 2010 (Figure 7) for Japan, for which the standardized index for quarter 4 is consistently larger than the nominal CPUE. Strong seasonality is shown is the estimated indices for the Japanese fleet (Figure 8), thus it is easier to visualize the indices separated by quarter. The indices for the two fleets show coincident values until about 2010. From 2005 to 2010, both indices increase. After 2010, the indices for the Korean fleet decline or stay stable in all quarters except 4, where a slight increase is shown from 2015-2017. For the Japanese fleet, the indices increase after 2010, with the largest increase taken place in quarter 4, followed by quarter 1 and 3. For quarter 4, a strong decline from 2016 to 2018 is displayed by the index derived from the

Japanese fleet. The length-frequency data for both fleets are, in general, similar except for the decrease in average size shown after 2010, in quarter 4 for the Korean fleet and in quarters 1 and 2 for the Japanese fleet (Figure 9).

The indices for the Korean and the Japanese fleets show several similarities between them and with the index for the New Zealand fleet (Figure 10). All three indices show similar increases around 2002, followed by a decline and a new increase from 2005 on. From 2005 to 2010 there was an increase in the average size in the Japanese fleet, which may indicate a strong cohort that was passing through the fishery. After 2004, the New Zealand fleet showed a dramatic increase in the use of light sticks, from no use in 2002 to use in almost all set after 2004, and on the use of squid as a bait, from almost no use in 2002 to use in 60% of the sets or more (Finucci et al. 2021). It is expected that such technological advances would propagate rapidly among the fleets and may have been adopted by other fleets, such as the Japanese and Korean fleets for which this information is not available.

Both the Korean and Japanese indices show strong seasonality and have similar values until 2010. This seasonality is also strong in the New Zealand index. The increase in density in quarters 1 and 4, markedly after 2010, in areas towards the east indicates that seasonal movement may be taking place. The spatial distribution of density shows an increase in density towards the eastern boundary of the area right at the equator, estimated for both the Korean and Japanese data, which starts in the period 2010-2014 (Figure 11), and it strengthen after 2015, for quarters 1 and 4. According to the conceptual model for the swordfish population in the south EPO (SAC-12-07), the adults migrate towards reproductive areas in quarters 1 and 4 and move closer to the coast in quarters 2 and 3, to forage in the frontal areas of influence of the Humboldt current. The northern stock also migrates towards the equatorial areas (SAC-12-07) and maybe present in some seasons, most likely in the boral summer (quarters 2 and 3). These movements are in synchrony with the oceanographic currents, which may be responsible for the strong seasonality in the trends.

Despite the similarities in the indices, there are differences that are worth noting. After 2015, both the Japanese and Korean indices differ: they shown increase or stability, respectively, while the New Zealand index shows a strong decline. There are three hypotheses that could explain those differences: (1) changes in availability of swordfish to the New Zeland fleet in comparison with the Korean and Japanese fleets (2) biases caused by imputation with data from preferential sampling; (3) changes in catchability due to changes in gear through time; or (2). It seems that the three indices maybe indexing the same population until about 2015, after that there is a divergence. There was a strong El Niño in 2015 that may have expanded the warm waters into the eastern part of the EPO and brough changes to the ecosystem and may have changed the distribution of the population. The increase in density in the eastern area after 2015 may be due to that. For quarters 1,4 and to some extend 3, after 2013, the Korean index shows in general smaller values than the Japanese index. This may be in in part due to the different distribution of effort of the two fleets and how much the imputation for those years was based on samples coming from a restricted area with higher densities, when the distributions of the fleets are more concentrated than other years (Appendix 1). In quarter 4, the Japanese fleet is almost exclusively restricted to areas south of the equator and east of 140°W, which are areas of higher densities. By imputing values based on those areas to the whole region, the index maybe positively biased. The differences may also be because of changes in gear configuration that are not considered in the standardization. It is known that both fleets use light sticks, which are known to increase markedly the catchability for swordfish (*e.g.* Nguyen and Winger, 2019). It is unknown, however, when the use of light sticks expanded in the Japanese and Korean fleets, and how much they have been used, or whether light sticks have been used to increase the

catchability of the target fish, bigeye tuna, or swordfish or both, as there are no data available on the use of light sticks for these fleets. The New Zealand index was derived from a model that included the light-stick effect. If all three indices were from the same population, the lack of correspondence between them after 2015 may in part be explained by the lack of inclusion of the light-stick effect in the models for the Japanese and Korean data, which do not show the marked decline evident in the New Zealand index.

FUTURE WORK

The understanding of the dynamic and structure of the stock could benefit from extending the current CPUE analysis to include data from the Japanese fleets to the WCPO. Additionally, work on comparison of density estimated from dataset from other fleets and research on stock definitions should be done.

REFERENCES

Dunn, PK & Smyth, GK. 1996. Randomized Quantile Residuals. Journal of Computational and Graphical Statistics. 236-244.

Hartig, F. 2020. DHARMa: Residual Diagnostics for Hierarchical (Multi-Level /Mixed) Regression Models. https://cran.r-project.org/package=DHARMa.

Finucci, B., Griggs,L., Sutton,P.,Fernandez, D., Anderson, O. 2021. Characterisation and CPUE indices for swordfish (*Xiphias gladius*) from the New Zealand tuna longline fishery, 1993 to 2019. New Zealand Fisheries Assessment Report 2021/07

Francis, R.I.C.C. 2011. Data weighting in statistical fisheries stock assessment models. Canadian Journal of Fisheries and Aquatic Sciences **68**(6): 1124-1138.

Maunder, M.N., and Punt, A.E. 2004. Standardizing catch and effort data: a review of recent approaches. Fisheries research **70**(2-3): 141-159.

Maunder, M.N., Thorson, J.T., Xu, H., Oliveros-Ramos, R., Hoyle, S.D., Tremblay-Boyer, L., Lee, H.H., Kai, M., Chang, S.-K., and Kitakado, T. 2020. The need for spatio-temporal modeling to determine catch-per-unit effort based indices of abundance and associated composition data for inclusion in stock assessment models. Fisheries Research **229**: 105594.

Nguyen, K. Q, and Winger, P.D. 2019. Artificial Light in Commercial Industrialized Fishing Applications: A Review, Reviews in Fisheries Science & Aquaculture, 27:1, 106-126, DOI: 10.1080/23308249.2018.1496065

Thorson, J.T., 2019. Guidance for decisions using the Vector Autoregressive Spatio-Temporal (VAST) package in stock, ecosystem, habitat and climate assessments. Fish. Res. 210, 143–161. https://doi.org/10.1016/j.fishres.2018.10.013

Thorson, J.T., and Barnett, L.A.K. 2017. Comparing estimates of abundance trends and distribution shifts using single- and multispecies models of fishes and biogenic habitat. ICES Journal of Marine Science **74**(5): 1311-1321.

Thorson, J.T., and Kristensen, K. 2016. Implementing a generic method for bias correction in statistical models using random effects, with spatial and population dynamics examples. Fish. Res. 175: 66–74. doi:10.1016/j.fishres.2015.11.016. url: http://www.sciencedirect.com/science/article/pii/S0165783615301399

Thorson, J.T., Shelton, A.O., Ward, E.J., Skaug, H.J., 2015. Geostatistical delta-generalized linear mixed models improve precision for estimated abundance indices for West Coast groundfishes. ICES J. Mar. Sci.

J. Cons. 72(5), 1297–1310. doi:10.1093/icesjms/fsu243. http://icesjms.oxfordjournals.org/content/72/5/1297

Xu, H., Lennert-Cody, C.E., Maunder, M.N., and Minte-Vera, C.V. 2019. Spatiotemporal dynamics of the dolphin-associated purse-seine fishery for yellowfin tuna (Thunnus albacares) in the eastern Pacific Ocean. Fisheries research **213**: 121-131

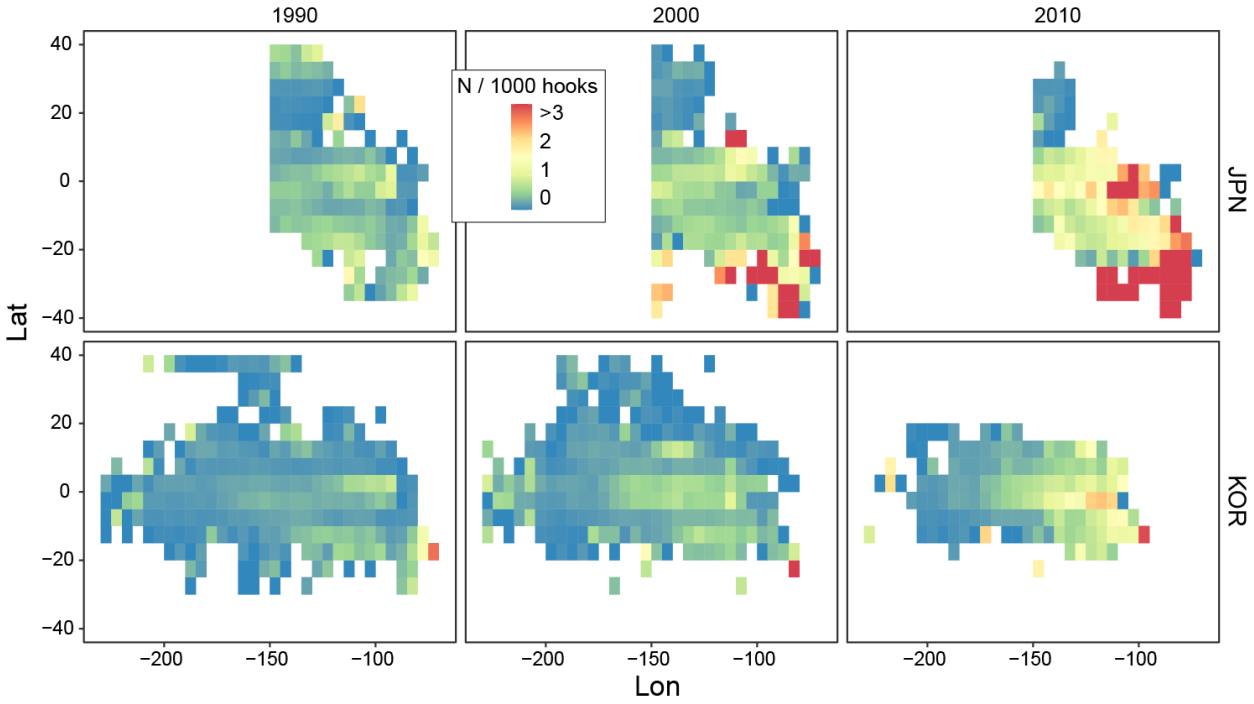

FIGURE 1. Nominal CPUE in number of swordfish per 1000 hooks from the data available for this study for Japan and Korea by decade (1990: 1994-1999, 2000: 2000-2009, 2010: 2010-2018). Note that no data west of 150°W is available for Japan.

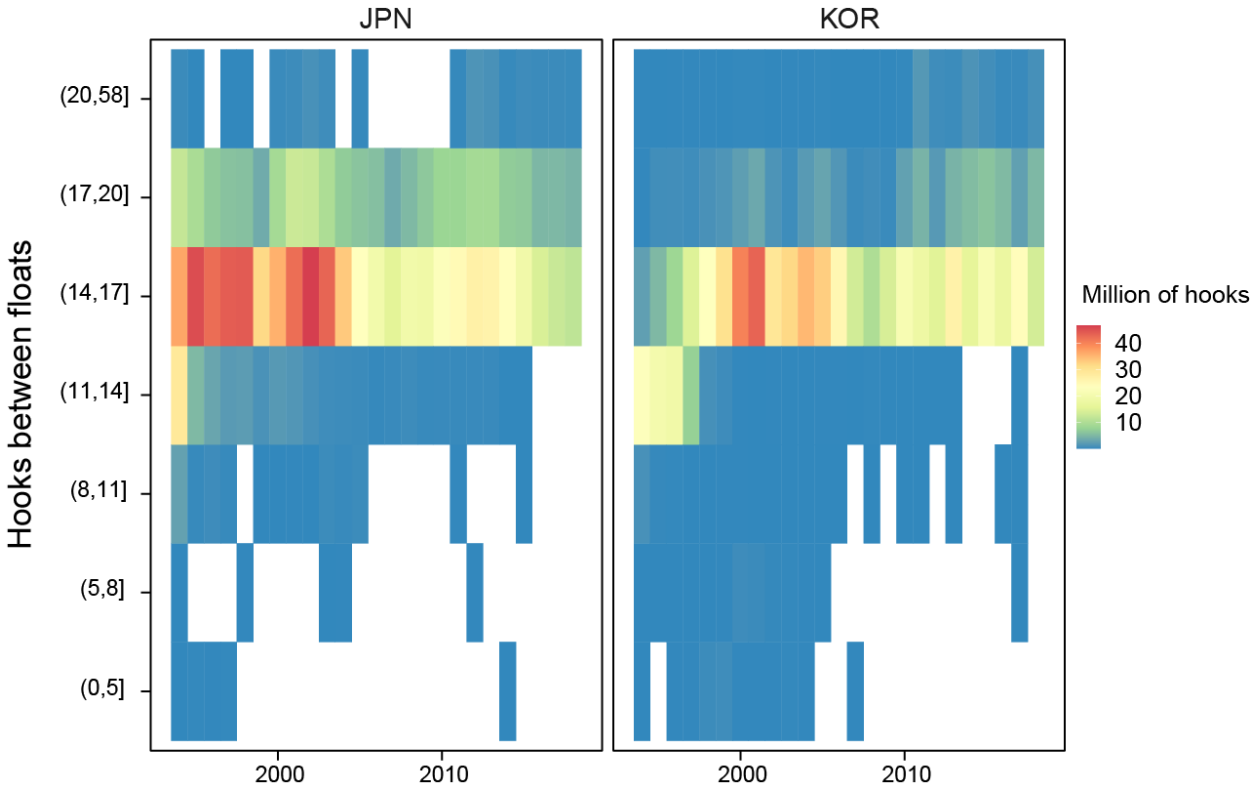

FIGURE 2. Effort by hooks between float categories for Japan and Korean in the study area (150°W to 110°W, 10°N to 15°S)

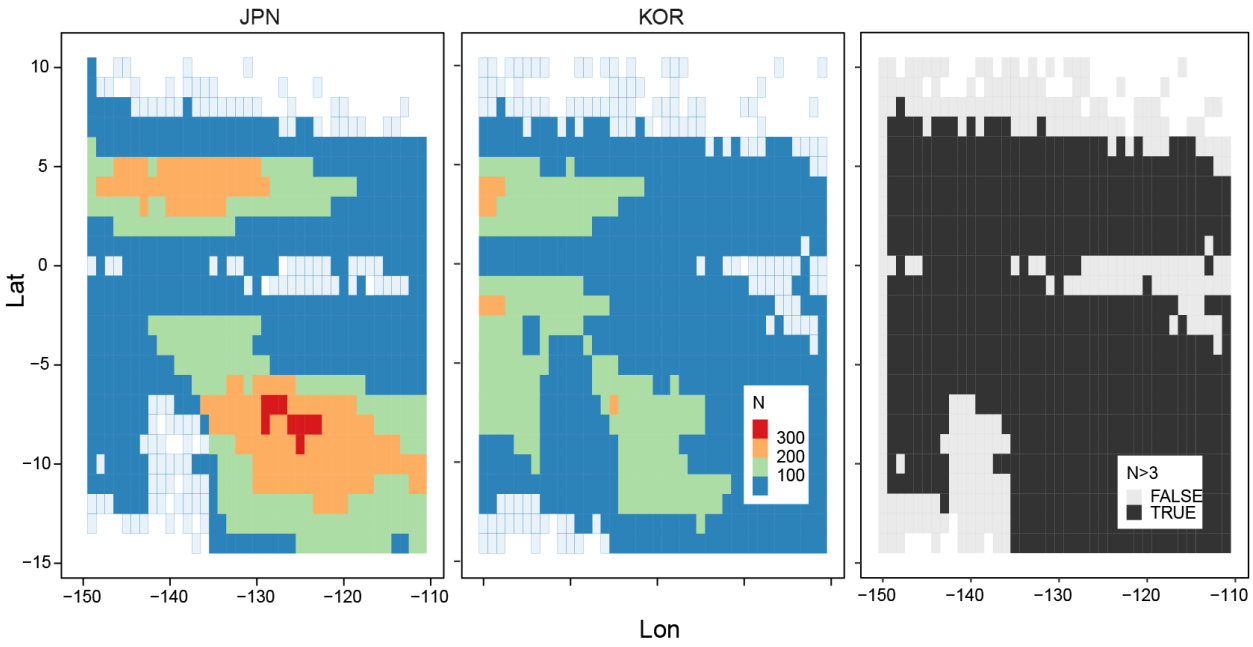

FIGURE 3. Right: distribution of cells with more or less than 3 observations (N, months x HBF categories) of data for Japan and Korea. Left: spatial domain of the spatiotemporal models.

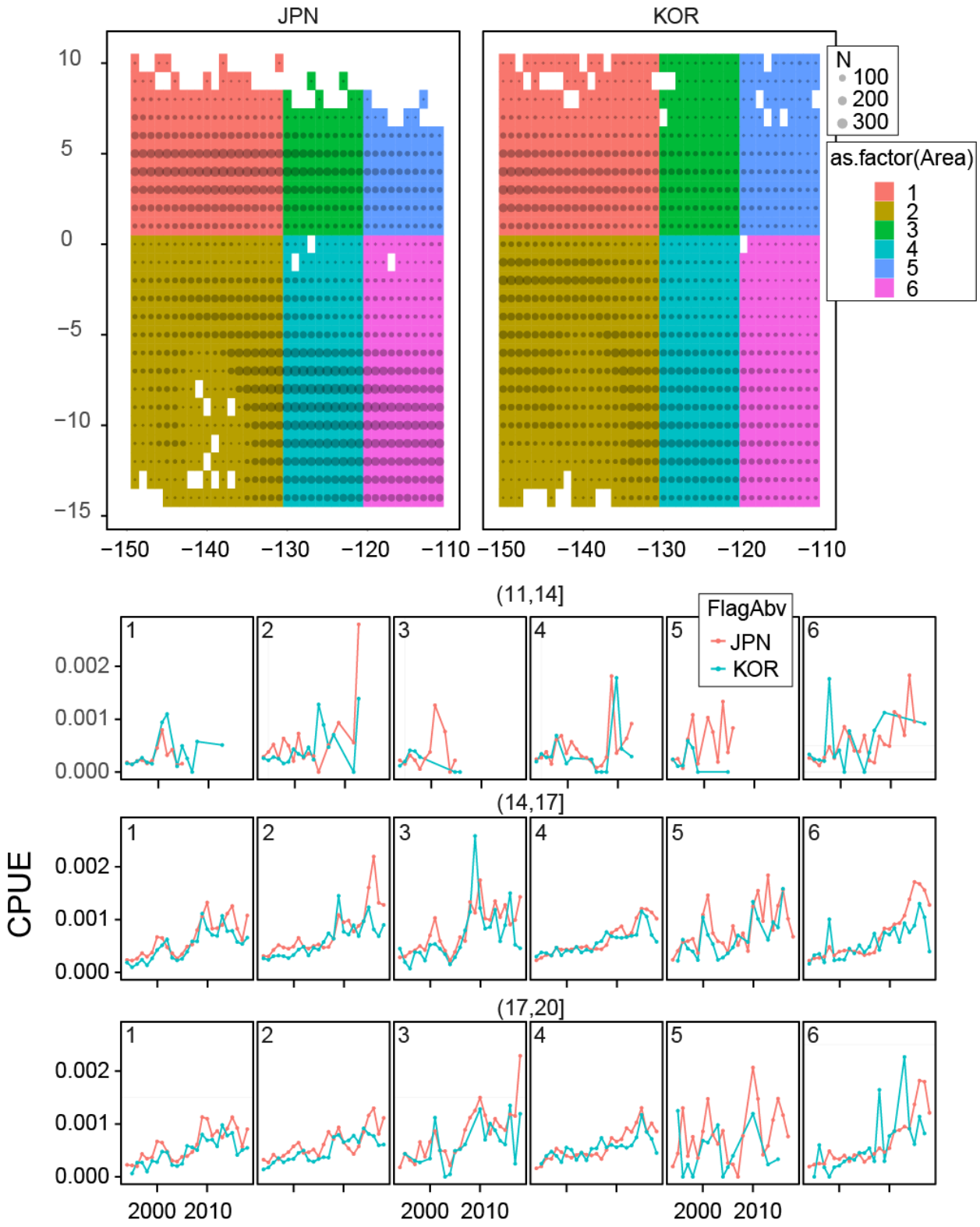

FIGURE 4. Top: number of cells (N, months x HBF categories) with data by area and fleet, Bottom: nominal CPUE in numbers per hook for Korea and Japan for four subareas within the study area.

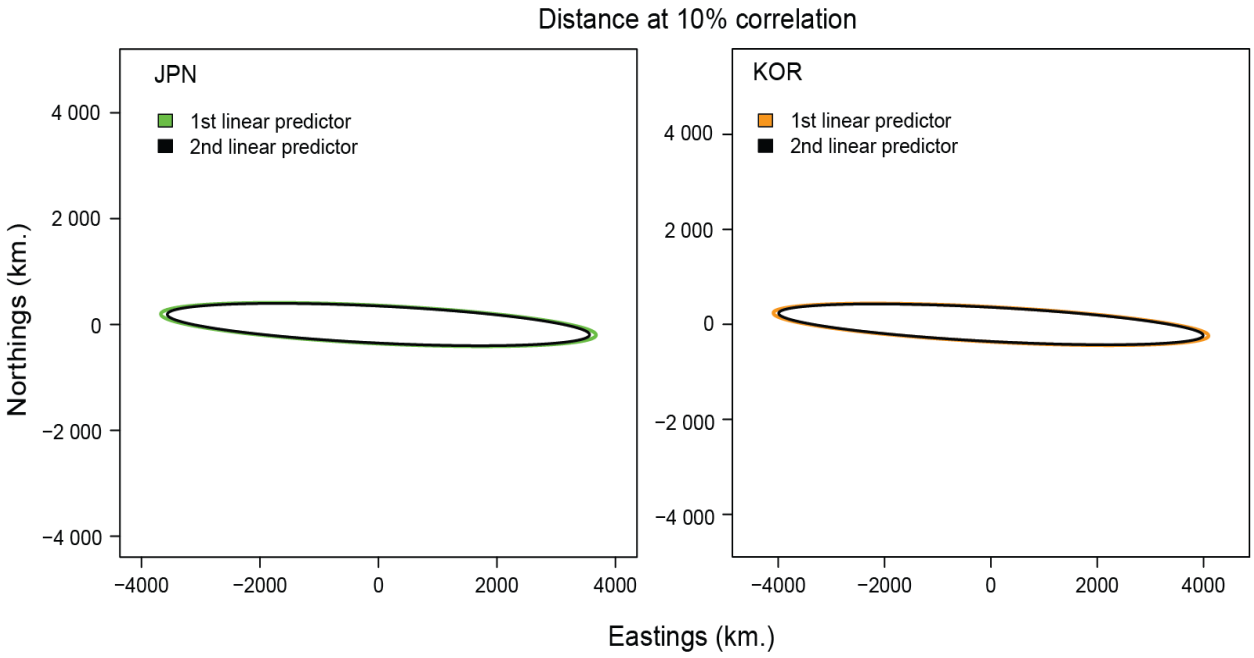

FIGURE 5. Spatial correlation estimated from the spatiotemporal models for Korea and Japan.

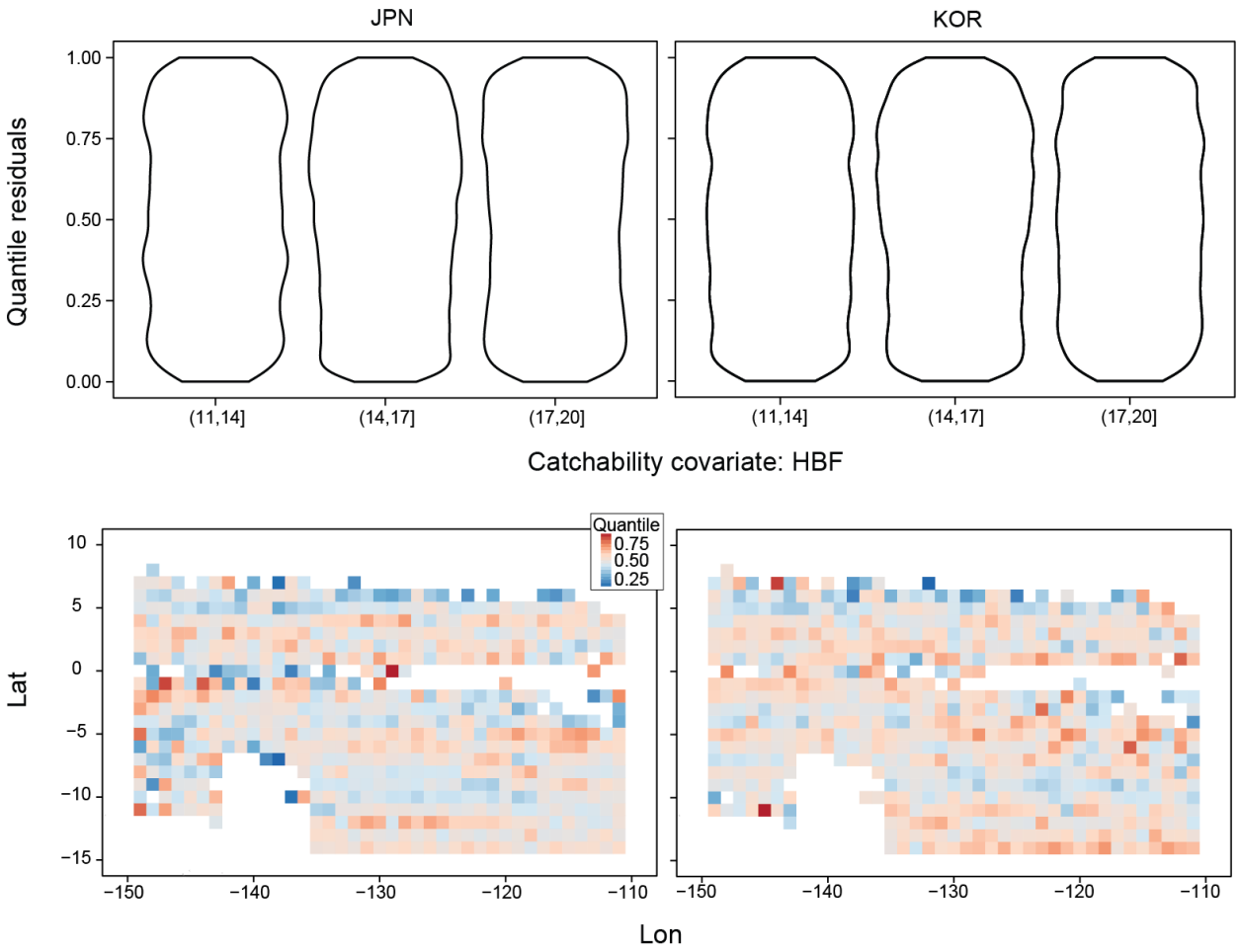

FIGURE 6. Top: violin plot of the quantile residuals for each category of the catchability covariate. Bottom: Median of the quantile residuals for each 1° by 1° cell.

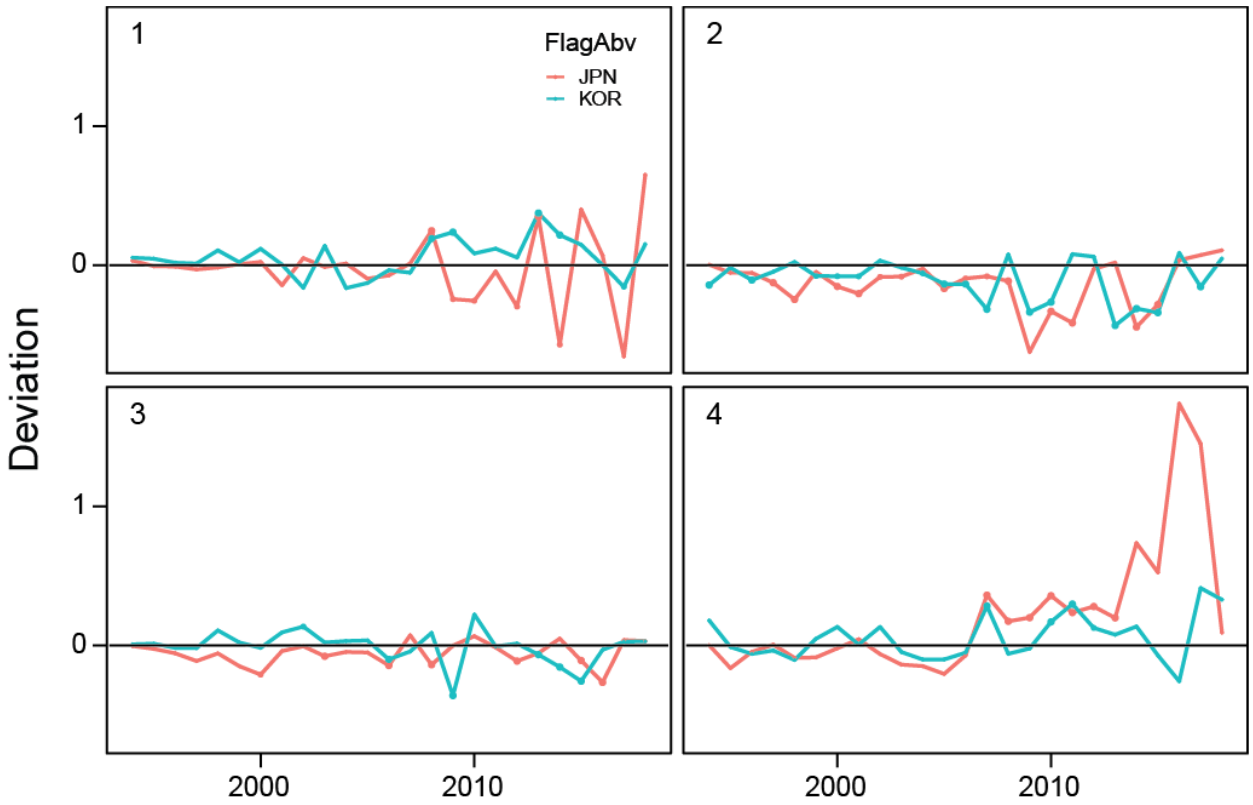

FIGURE 7. Difference between the standardized indices and the nominal CPUE for Korea and Japan by quarter.

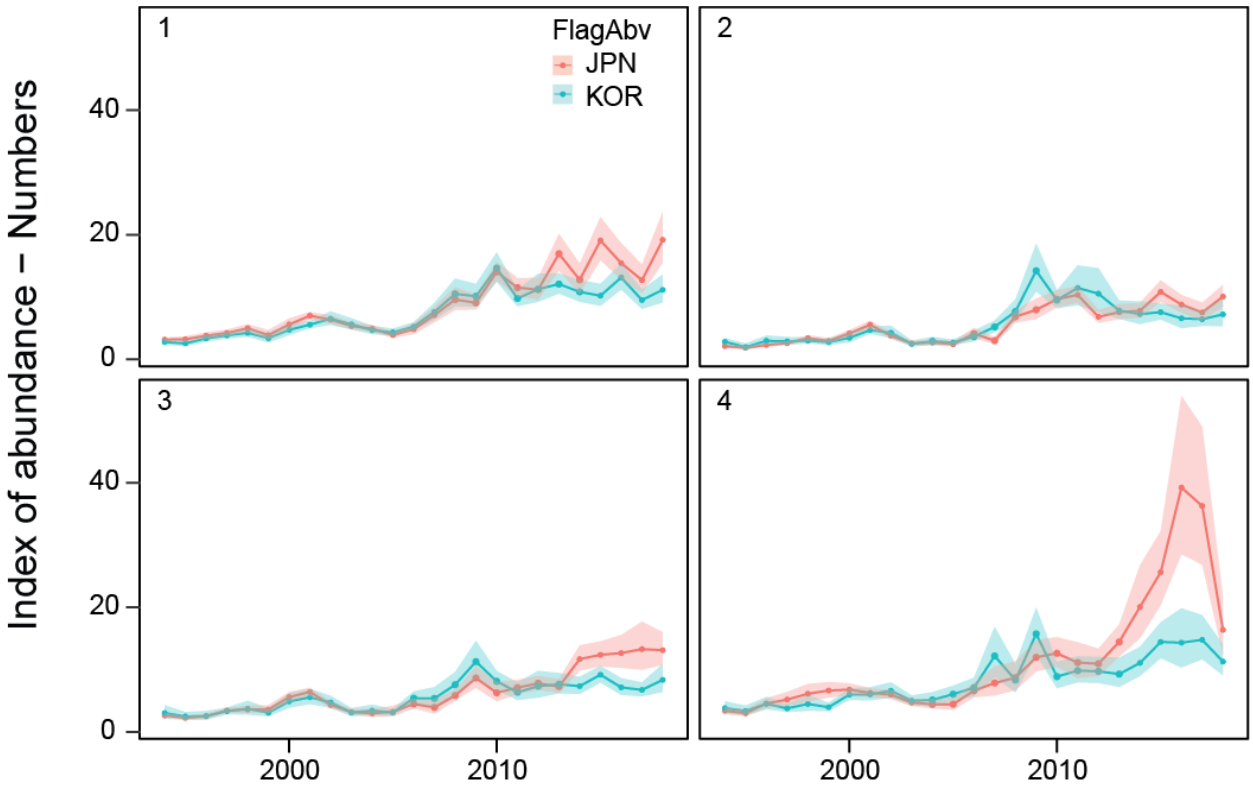

FIGURE 8. Standardized indices of abundance by for Korea and Japan by quarter.

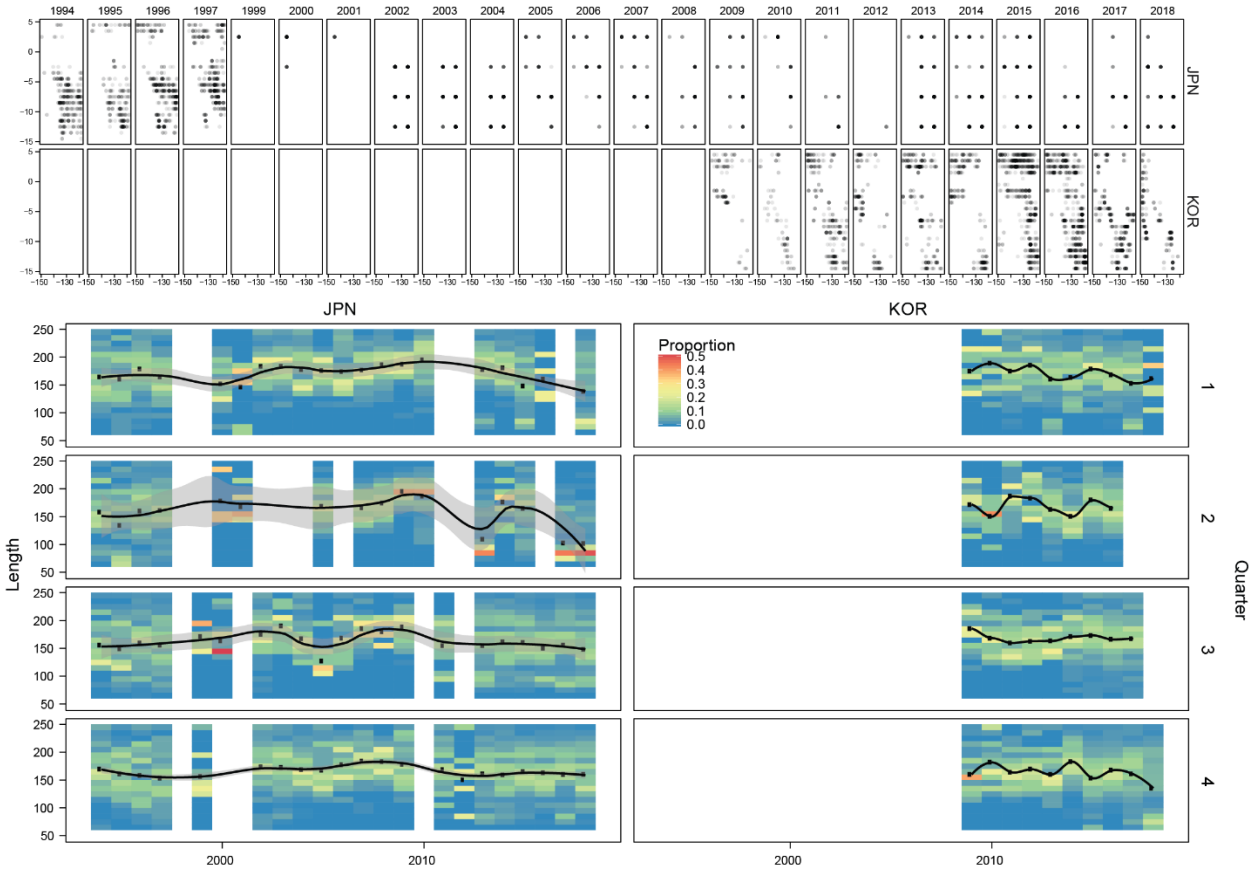

FIGURE 9. Top: Locations of the length-frequency data in the equatorial area by year and fleet. Bottom: Length frequency distributions for the Japan and Korean fleets in the equatorial area, with mean length and a smooth lowess curve (s=0.4) on mean length.

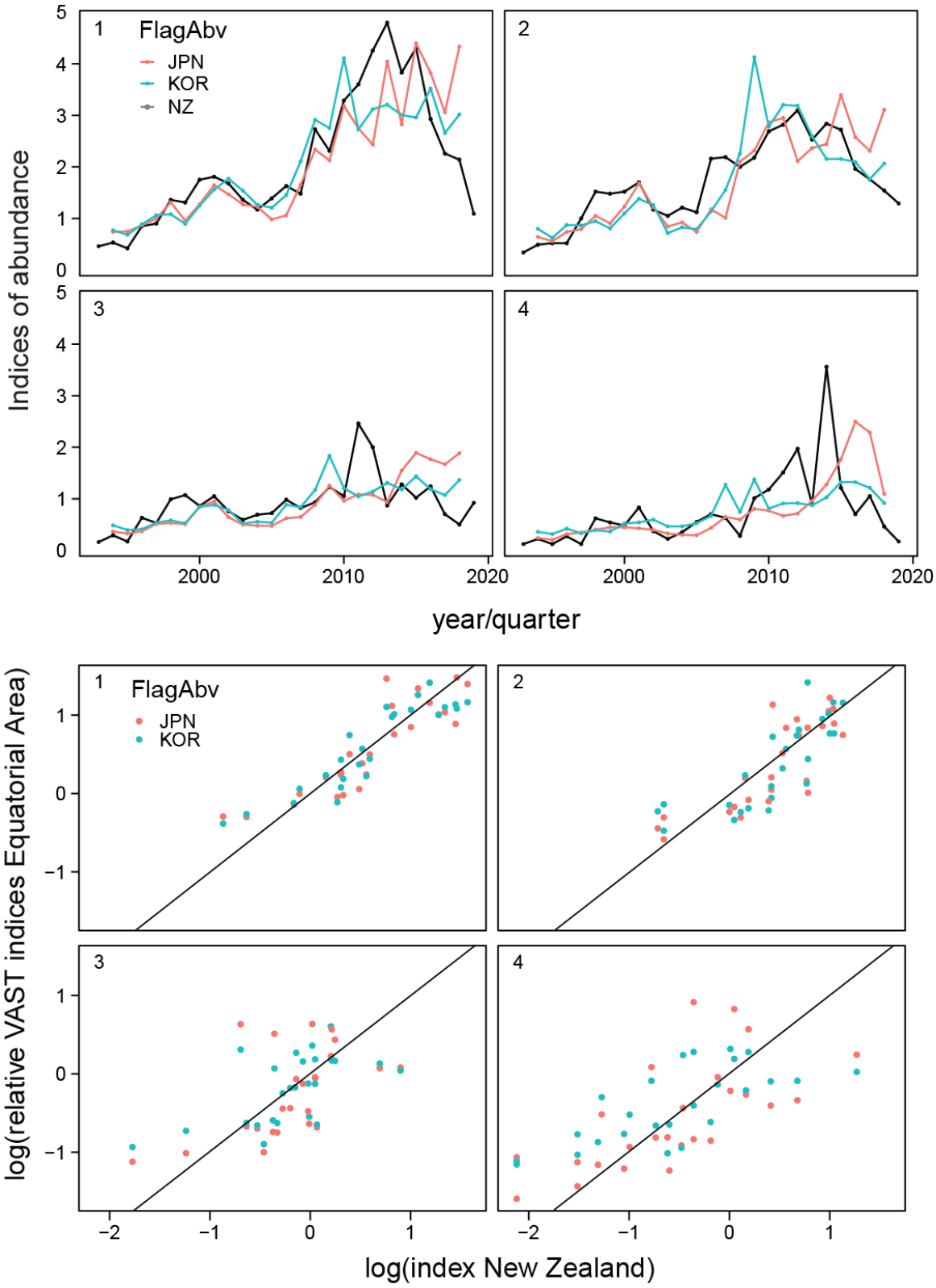

FIGURE 10. Comparison with the index obtained from the New Zealand fleet. The indices were transformed so they have the same mean as the New Zealand index by quarter,

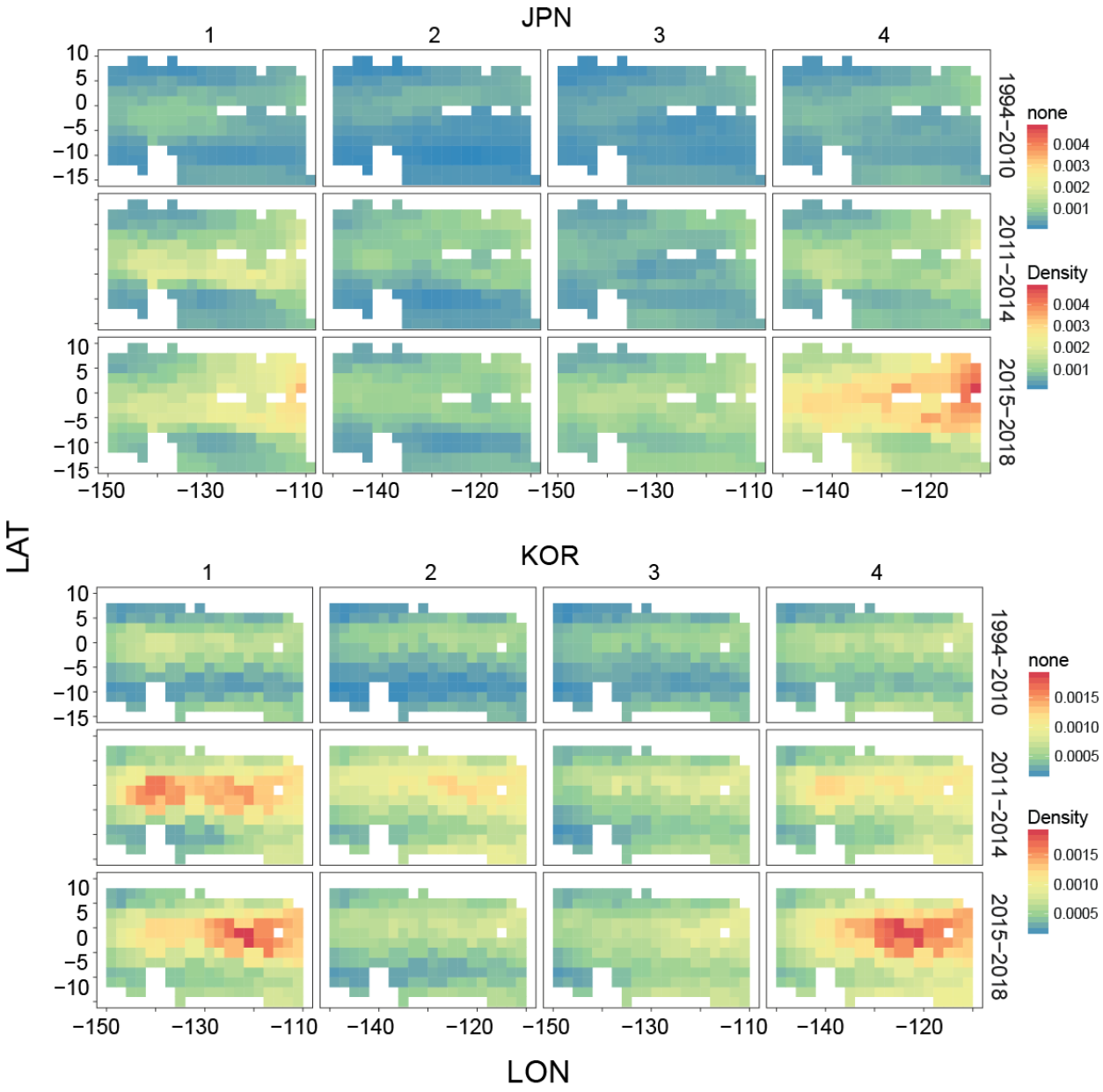

FIGURE 11. Map of estimates for Korea and Japan, by quarter and period (1994-2010,2011-2014,2014-2018)

APPENDIX 1

FIGURE A-1. Maps of median quantile residuals for Korean and Japan by quarters

TABLE 1. Indices of abundance for swordfish in the equatorial area of the EPO (150°W to 110°W, 10°N to 15°S) obtained from longline CPUE for Japan and Korea standardized using spatiotemporal models.

Year	Quarter	Index (JPN)	CV (JPN)	Index (KOR)	CV (KOR)
1994	1	3.142	0.048	2.373	0.075
1995	1	3.159	0.063	2.102	0.098
1996	1	3.669	0.064	2.728	0.073
1997	1	4.216	0.058	3.274	0.062
1998	1	5.556	0.055	3.335	0.085
1999	1	4.051	0.091	2.759	0.112
2000	1	5.403	0.072	3.850	0.091
2001	1	6.967	0.037	4.807	0.048
2002	1	6.226	0.046	5.456	0.074
2003	1	5.378	0.046	4.746	0.072
2004	1	5.187	0.052	3.894	0.063
2005	1	4.154	0.050	3.719	0.057
2006	1	4.484	0.081	4.477	0.058
2007	1	6.995	0.074	6.497	0.078
2008	1	9.893	0.078	8.982	0.097
2009	1	9.013	0.057	8.490	0.082
2010	1	13.483	0.049	12.674	0.075
2011	1	11.643	0.054	8.402	0.056
2012	1	10.302	0.071	9.616	0.100
2013	1	17.134	0.082	9.891	0.061
2014	1	11.965	0.086	9.273	0.074
2015	1	18.633	0.083	9.121	0.076
2016	1	16.203	0.079	10.854	0.069
2017	1	12.964	0.072	8.197	0.066
2018	1	18.361	0.099	9.304	0.097
1994	2	2.112	0.062	2.264	0.101
1995	2	1.836	0.074	1.768	0.139
1996	2	2.429	0.068	2.476	0.120
1997	2	2.607	0.053	2.456	0.106
1998	2	3.463	0.064	2.688	0.079
1999	2	2.982	0.066	2.289	0.093
2000	2	4.048	0.054	3.120	0.115
2001	2	5.520	0.047	3.919	0.061
2002	2	4.014	0.057	3.582	0.113
2003	2	2.776	0.061	2.029	0.093
2004	2	3.036	0.082	2.353	0.102
2005	2	2.427	0.074	2.241	0.073
2006	2	3.871	0.083	3.230	0.111
2007	2	3.325	0.080	4.414	0.080
2008	2	6.914	0.066	6.410	0.114
2009	2	7.627	0.085	11.733	0.135

2010	2	9.429	0.058	7.889	0.069
2011	2	9.708	0.061	9.101	0.138
2012	2	6.953	0.059	9.055	0.165
2013	2	7.789	0.069	7.362	0.084
2014	2	8.039	0.064	6.120	0.122
2015	2	11.173	0.065	6.119	0.075
2016	2	8.484	0.075	5.951	0.116
2017	2	7.608	0.089	5.013	0.082
2018	2	10.232	0.081	5.863	0.143
1994	3	2.522	0.068	2.513	0.177
1995	3	2.262	0.062	2.043	0.129
1996	3	2.555	0.076	2.122	0.138
1997	3	3.548	0.052	2.779	0.069
1998	3	3.671	0.080	3.012	0.161
1999	3	3.508	0.083	2.723	0.106
2000	3	5.818	0.063	4.387	0.107
2001	3	6.570	0.045	4.578	0.097
2002	3	4.455	0.060	4.057	0.099
2003	3	3.458	0.062	2.696	0.096
2004	3	3.309	0.091	2.875	0.119
2005	3	3.282	0.119	2.777	0.077
2006	3	4.310	0.074	4.597	0.086
2007	3	4.478	0.124	4.345	0.149
2008	3	6.123	0.070	6.092	0.115
2009	3	8.697	0.090	9.531	0.130
2010	3	6.657	0.101	6.261	0.088
2011	3	7.518	0.073	5.429	0.106
2012	3	7.462	0.063	5.925	0.145
2013	3	6.496	0.067	6.808	0.103
2014	3	10.730	0.069	6.141	0.089
2015	3	13.123	0.070	7.458	0.060
2016	3	12.260	0.100	6.165	0.080
2017	3	11.583	0.116	5.567	0.077
2018	3	13.076	0.089	7.086	0.126
1994	4	3.570	0.077	3.285	0.126
1995	4	3.045	0.080	2.908	0.112
1996	4	4.698	0.084	3.864	0.105
1997	4	5.175	0.100	3.037	0.077
1998	4	6.011	0.116	3.593	0.143
1999	4	6.672	0.082	3.352	0.079
2000	4	6.655	0.066	4.770	0.077
2001	4	6.392	0.050	4.989	0.081
2002	4	5.902	0.054	5.481	0.086
2003	4	4.852	0.057	4.269	0.073

2004	4	4.477	0.074	4.287	0.103
2005	4	4.368	0.101	4.830	0.096
2006	4	6.510	0.076	6.163	0.094
2007	4	9.692	0.125	11.721	0.160
2008	4	8.936	0.110	6.858	0.139
2009	4	12.068	0.096	12.685	0.123
2010	4	11.521	0.093	7.467	0.109
2011	4	10.004	0.108	8.387	0.102
2012	4	10.700	0.092	8.442	0.104
2013	4	14.380	0.078	8.050	0.120
2014	4	19.156	0.139	9.468	0.096
2015	4	26.483	0.113	12.192	0.082
2016	4	37.444	0.161	12.207	0.145
2017	4	34.280	0.153	11.168	0.108
2018	4	16.351	0.126	8.441	0.096